Preparing the operation of Wendelstein 7-X in the steady-state regime

H.-S. Bosch, P. van Eeten, O. Grulke, T. Bräuer, S. Degenkolbe, M. Nagel, T. Rummel, J. Schacht, A. Spring, A. Winter, W7-X Team

Max-Planck-Institut für Plasmaphysik, 17491 Greifswald, Germany

A B S T R A C T

The Wendelstein 7-X stellarator (W7-X) started operation in December 2015 and has performed three experimental campaigns up to November 2018. Since then the device has been completed to the planned configuration (most importantly with predominantly actively cooled first wall, including the High Heat Flux divertor and a divertor cryo pump) to be able to perform stationary plasma programs. After this completion pFhase, at the end of 2021, the commissioning has been performed and scientific operation has started in the fall of 2022.

1. Introduction

The numerically optimized stellarator Wendelstein 7-X [1], is a superconducting device set up at Greifswald [2] and has started operation [3] in December 2015 as a limiter experiment [4] reaching a record value in the fusion triple product Nτ for stellarators [4,5,6]. For the second and the third phase, an inertially cooled divertor has been installed, allowing for an energy input of 200 MJ [7]. This has allowed extensive divertor studies, including first detached divertor plasmas for more than 30 seconds [4]. However, all the discharges were limited by the restrictions in the energy input. To go beyond this restriction, the inertially cooled divertor had to be replaced by a steady-state cooled divertor and several components of the inner wall elements were modified.

Stellarator optimization is emerging as a powerful approach to attain favorable plasma conditions by a special shaping of magnetic fields. It is advantageous that plasma properties can be 'physically designed' by an appropriate arrangement of magnetic field coils [8]. This was facilitated by the invention of modular coils [9] which allowed to create modulations of the magnetic field that directly affect different aspects of the plasma behavior. In the field of plasma theory, most beneficial confinement is expected in so-called quasi-symmetric configurations [10]. W7-X is optimized to reduce neoclassical losses and currents and to keep feasible coils and a divertor solution [1]. The initial results of W7-X have led to incorporate even other optimization targets and to develop more refined procedures for the technically complicated task of an optimized physics design of a stellarator [11].

After describing some physics results, obtained until 2018, the new components and their installation will be described. After this completion of W7-X at the end of 2021, technical commissioning started in January 2022 and physics commissioning in September 2022. Highlights of the technical commissioning will be reported at the end.

2. Experiments on stellarator optimization

The mission of Wendelstein 7-X is to explore the fundamental properties of optimized stellarators providing plasmas in optimized stellarator fields. Thereby, the assessment of the reactor capabilities in 3D magnetic fields came into reach. To this end, high beta values and low collisionalities are required to attain the impact of 3d MHD stability as well as neoclassical physics in the long-mean-free-path regime [12]. In terms of control parameters, these studies need high-density operation at high heating power thus defining the heating, fueling and exhaust requirements. A crucial element is safe divertor operation with detached plasmas [13]. At the same time, an important advantage of stellarators is their capability for steady-state operation since poloidal fields are generated by external coils. W7-X is equipped with superconducting coils installed to allow very long pulse lengths. The longest time-scales are set by the L/R times for the plasma response to bootstrap currents (for high performance plasmas in the order of some ten seconds) and thermal equilibration (in the order of seconds). First experience with long-pulse operation, for instance, shows impurity release after about two minutes of operation [13]. To meet with the mission goals of W7-X, therefore, the operational capabilities of W7-X need to integrate high heating power and very long pulse lengths, technically up to 30 minutes.

As usual for stellarators, the magnetic field to confine the plasma is performed by coils external from the Plasma vessel. Wendelstein 7-X has a superconducting coil system, built up from 50 non-planar coils (10 coils in 5 types, numbered 1 to 5) and 20 planar coil (10 coils in 2 types, A and B). The seven types of coils are powered by 7 individual power supplies, i.e. the seven coil systems can be fed independently from each other [14]. However, as the coils interact on each other by electromagnetic forces, the coil system has to be strongly supported by different support elements [15,16,17]. All superconducting coils are fixed to a central support ring. This structure is made up of ten identical welded

segments that are bolted together to form a pentagon-shaped ring of five modules. Each of the 70 coils is fixed radially inwards to the support ring in two points. The magnetic forces acting between the non-planar coils are taken by inter coil support elements. On the inner side of the torus, where the distance between coils is small and accessibility is limited, the so-called narrow support elements are placed. On the outboard side of the torus, the so-called lateral support elements are installed. The planar coils are supported via stainless steel arms, called planar coils support, against the non-planar coils.

With seven types of coils (i.e. seven degrees of freedom), the flexibility is much larger than what was used for the design, and can hardly be visualized in a 3d-view. Only a reduced view on this configuration space is possible in a 3d-figure [18]. In Fig. 1, the center of the graph stand for the "Standard configuration" where the currents in all non-planar coils are the same ($I_1 = I_2 = I_3 = I_4 = I_5$) and the planar coils are switched off ($I_A = I_B = 0$). Along the X-axis the relation between the non-planar coil can be varied (as indicated in Fig. 1), resulting in a variation of the mirror-ratio (B_{max}/B_{min}) in one module, as can be seen in the icons.

In the Y- and Z-axis, also the planar coils carry currents, in a limited version of all possible current combinations. Along the Z-axis, the Iota at the plasma edge is varied, along the Y-axis the plasma is shifted radially.

Meanwhile, also many new magnetic configurations have been proposed, and for each of these configurations, a structural assessment is required. For these assessments, the coils and the support structure were modelled by 3d-FEM models. Each magnetic configuration is defined by a set of seven coil current, used as input for the 3d-FEM model, which calculates deformation of coils, clashes of coils, tension in screws. Based on these analyses, magnetic configuration can be accepted or rejected for operation [19,20]. Also the seven power circuits have some electrical interactions, depending on the currents, which is also taken into account in this procedure.

One example of the impact of the magnetic configuration is shown in Fig. 2 [21]. This example proves that the optimization concept works as for minimizing plasma currents. The waveforms and reference values (horizontal lines with error margins in Fig. 2, I_{BS}^{∞}) show measurements of the plasma shielding current evolution and calculations of the expected, stationary bootstrap current. The color refers to two different magnetic configurations attained by powering or switching-off one type of the planar coils (indicated by I_B/I_A). This difference in one of the seven coil current settings results in a higher toroidal magnetic mirror which directly affects the fraction of mirror-trapped particles. Neoclassical theory, a major ingredient in the optimization of W7-X, predicts two main results: first, the bootstrap current is as smaller than in an equivalent tokamak and results in no more than few kA for the plasmas underlying Fig. 2. Second, just the change of mirror trapped particles leads to smaller currents for the lower toroidal mirror case. This is indicated by neoclassical bootstrap current calculations from plasma profile measurements as shown in Fig. 2. Likewise, the L/R-response of the internal plasma shielding current is seen as the rise of the measured plasma current in Fig. 2. The results show that the predicted ratio of currents in those two configurations match perfectly and with deviation of less than 1kA also in terms of the expected, absolute saturation value of the rising waveforms in Fig. 2. This comparison of measured plasma currents with theoretical predictions emerging from neoclassical theory provides the first confirmation of the basic concept of stellarator optimization in W7-X.

Other important results clearly show the optimization of W7-X, like the improved confinement [6] or the ideal magnetic configuration with closed magnetic flux surfaces, which also shows the exact mounting of the magnet system [22], and successful divertor discharges [7].

3. Completion of W7-X

Between November 2018 and January 2022, W7-X was completed to the reference design, i.e. being able to perform long-pulse operation with high heating power. Therefore the power and particle exhaust had to be improved with a steady state divertor and wall, the corresponding water cooling and cryo pumps in the divertor area.

3.1. In-vessel components

Design and constructed of the in-vessel components started in the early 2000s [23], based on CFC for most of the target plates (loaded up to 10 MW/m^2), fine grain for the lower loaded heat shield (inner side of the vessel, < 500 kW/m^2) and stainless steel panels on the outer side (< 200 kW/m^2) [24].

The installation of these actively cooled components (Water) was the focus of this completion. The 120 divertor modules (up to 70 kg) had to be assembled in the rather tight vessel with high precision of 0.2 mm, see Fig. 3. The walls are covered by 8000 carbon tiles installed on water-cooled heat sinks. The second challenge was posed by the connections between the divertor modules to the cooling pipes (about 7 km of pipes in the vessel). In 40 feed throughs these internal water pipes were

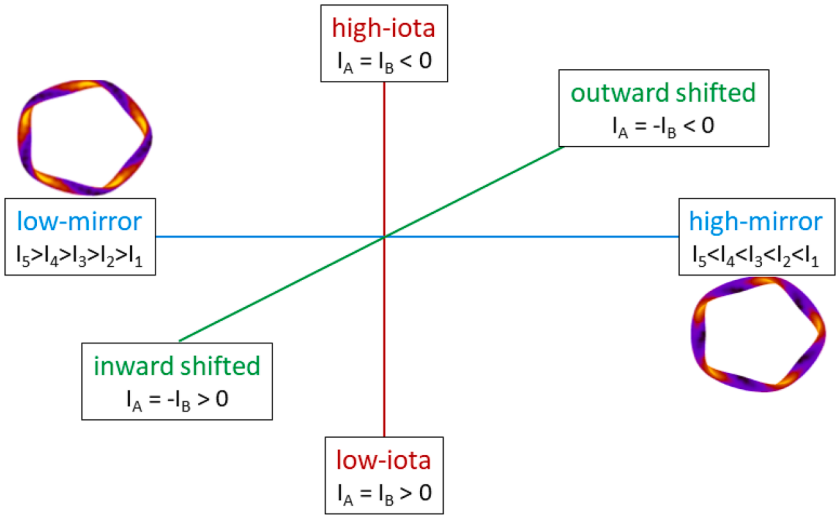

Fig. 1. Simplifies magnetic configuration space. With 7 independent magnetic coils, boundary conditions have to be made to be able to describe the configuration in 3d space. The fully optimized configuration ("standard configuration") has identical current in all non-planar coils. Modifying these currents changes the depth of the mirror ratio in a module, as shown in the little icons. Powering also the planar coils, iota at the plasma edge and the radial position can be varied.

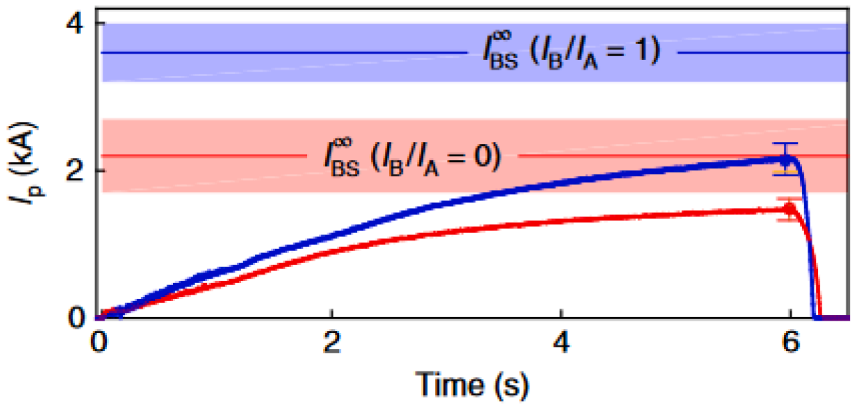

Fig. 2. Comparison of the measured plasma current with the total stationary neoclassical bootstrap current I^{∞}_{BS}. The shaded areas show error estimates from uncertainties in the profile measurements entering the neoclassical modelling [21]

Fig. 3. In this situation, a worker installs a Vertical Divertor module, supported by a position device. Positions for the later assembly of Horizontal Modules, baffles and Heat shields are visible

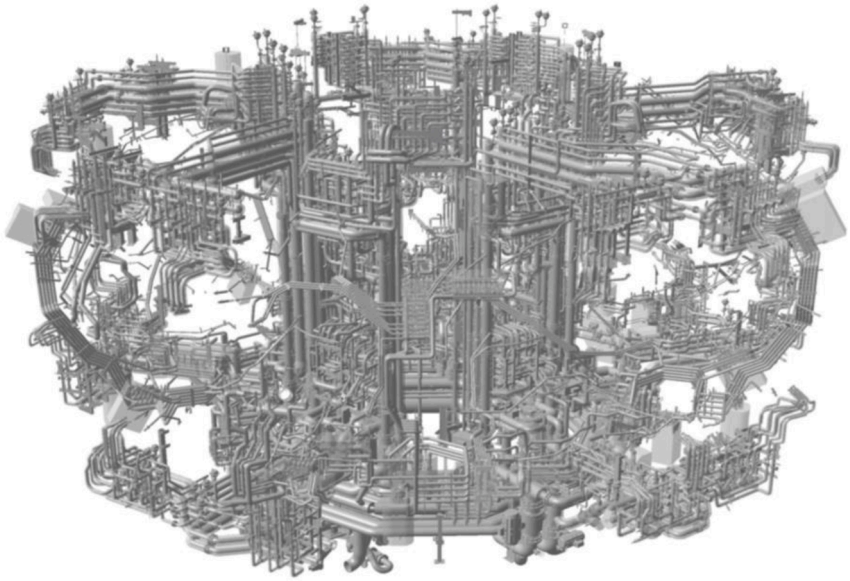

Fig. 4. 3d-model of the Water cooling pipes on W7X for target, baffle and wall circuits, port liner and diagnostic cooling. W7-X is not shown here.

connected to the external water cooling (see next chapter). The extremely tight installation space behind the divertor required the adaption of hundreds of small pipes, supports and interfaces. New, space-saving tools and procedures had to be developed and were tested at a mock-up of the plasma vessel. To minimize the risk of water leaks all connections were leak-tested at 10^{-9} mbar l/s.

Also ten divertor cryo pumps have been installed behind the divertor, which requires lN_2 and Helium (see chapter 3.3) for pumping, but also water cooling for the room temperature chevron (RT-Chevron, (see chapter 3.2).

3.2. Water cooling

To provide the water-cooling for the above mentioned components, an extensive network has been installed around W7-X, see Fig. 4. This System consists of 4 primary systems to cool the in-vessel components (Target, Baffle, wall, port liners and diagnostic, plasma vessel and ports and heating). Part of the port cooling is also the cooling of the RT Chevron, which has to be stopped and drained in the event of failure of the water cooling: This is a SIL-2 safety function to avoid freezing of this cooling lines.

This system was largely designed and manufactured in-house, as the rather complex cycle of design, fabrication and assembly had to be performed in a rather tight space. This required short ways between the involved groups. This network has now ca. 657 circuit in the torus hall, with about 550 volume flow and temperature sensors. All these electric components had been tested for their functionality in magnetic fields. Total length of the pipes is about 6,5km in different sizes (diameter 10-250 mm). The pressure in these circuits in operation is 12-18bar (dynamic) and 2-20bar (static) and the temperature at the inlet is 25-30°C (allowing a swing 55°C).

The commissioning of the cooling water system required thorough leak and pressure testing, filling, manual hydraulic balancing between different pipes, as well functional testing. Although no leaks have been detected, these tasks took more than 6 months.

3.3. Cooling of the divertor cryo pump (CVP)

Behind the divertor units in all 10 half modules, 10 cryo pumps had been installed, that will be used for the density control in hydrogen plasma. The cryo pumps are cooled with supercritical helium with an inlet temperature of 3.9 K and a total mass flow rate of 250 g/s. In addition a thermal shield protects the cold panels of the cryo pumps from thermal radiation from the warm plasma vessel walls and from the plasma itself. The thermal shield is cooled with liquid nitrogen. Cold helium and liquid nitrogen are supplied from the refrigerator hall with a 50 m long multi-channel vacuum insulated transfer line (HTL) to a distribution box (CVB) in the basement of the torus hall, see Fig. 5. From there, 10 multi-channel lines (KTL) connect the valve box with the nozzles of the dedicated supply port in each half module. More details on the CVP and on the cooling concept are given in [25,26].

As the design space in the center of the torus hall was already crowded is was difficult to find a pipe routing for the vacuum insulated transfer lines [27]. The functional requirements plus the assembly needs (specifically for the in-situ welding seams) were difficult to achieve. The 3-D routing in Fig. 5 gives an impression of the design task.

The single pipes of the transfer lines were fabricated, pressure tested and leak tested with cold helium in industry before the pipes were shipped to IPP. The same testing was done for the CVB. Assembly started with the pipes of the KTL and HTL followed by the valve box. The HTL pipes were threaded into the pipe shaft one by one and then connected. The connection sequence contained the welding of the process pipes, cold shock testing of the welding seams followed by a leak test with helium. Then superinsulation was wrapped around the pipes in the connection area, the thermal shield was closed and finally the vacuum shell was welded. The welding seam of the vacuum shell was also leak

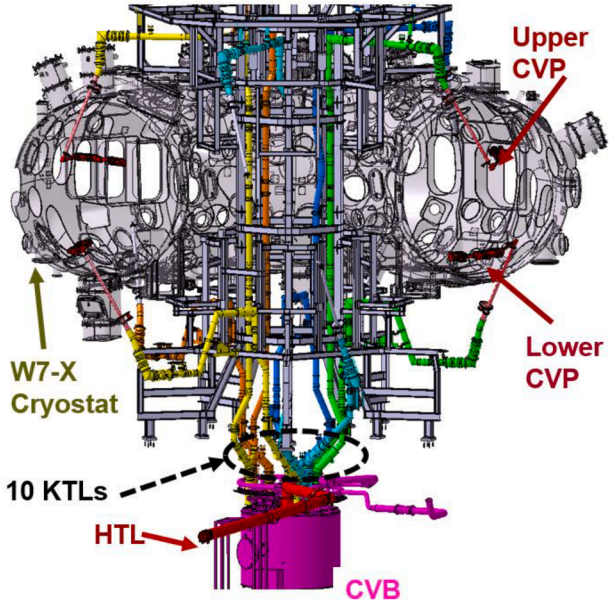

Fig. 5. CAD-snapshot of the cryostat vessel, the cryo valve box (CVB) the multi-channel-transfer lines (KTL). Those lines connect the valve box with the cryo-pump nozzels at the cryostat shell.

tested. Part of these connections were done at predefined locations before the pipes were finally positioned. This was required because welding was not possible for all pipes at the final position. Similar working steps were required for the 10 KTL. Fig. 6 shows the process lines of a KTL that are enclosed by a copper thermal shield before the lines are threaded in the vacuum shell.

In a next work step the tightly packed valve box (see Fig. 7 left) was put in position on site (see Fig. 7 right). All transfer lines were then welded to the valve box interfaces. These steps were followed by the connection of the 10 KTL to the port nozzles. Here as well process pipe connections were shock cooled and helium leak tested. Once after all welding was done, a pressure test and an integral helium leak test was carried out. Finally a function test of the box was done with the connected transfer lines.

3.4. Data acquisition for W7-X

The CoDaC division integrated more than 30 new or significantly enhanced diagnostic systems, nearly doubling the number of previously supported systems. In previous experimental campaigns, a number of diagnostics could not be integrated into the central infrastructure and ran on a parallel control and archiving system based on MDSplus. Now an interface to the central infrastructure has been implemented, which allows a full integration of the component in terms of control, archiving and timing but leaves the data acquisition to the individual diagnostic. This will greatly facilitate experimental operation in OP 2.1, and the use of the MDSplus parallel infrastructure is discontinued.

The divertor protection system consists of more than 20 high-speed cameras of 4 different types which had to be implemented into the real-time control system of W7-X. In order to propose a standardized solution, a set of generic mTCA-based frame grabbers were developed, which can be configured via FMC add-on boards to interface to cameras conforming to Camera Link, Camera Link HS and CoaXpress camera interfaces while maintaining the identical programming API through a GeniCAM compatible driver implementation in the real-time control system. This allows the integration of any camera conforming to the aforementioned standard with little software effort and if the camera is compliant with the GenICAM standard, practically no additional software effort is required. It is also the ITER preferred solution for cameras.

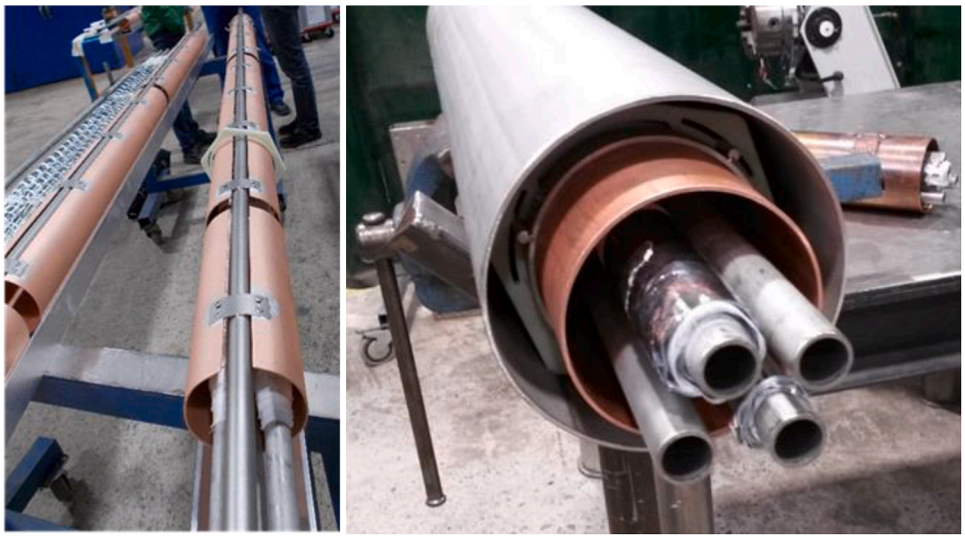

Fig. 6. Process pipes (for LN2 and Helium), the copper shield and vacuum jacket of a transfer line (KTL)

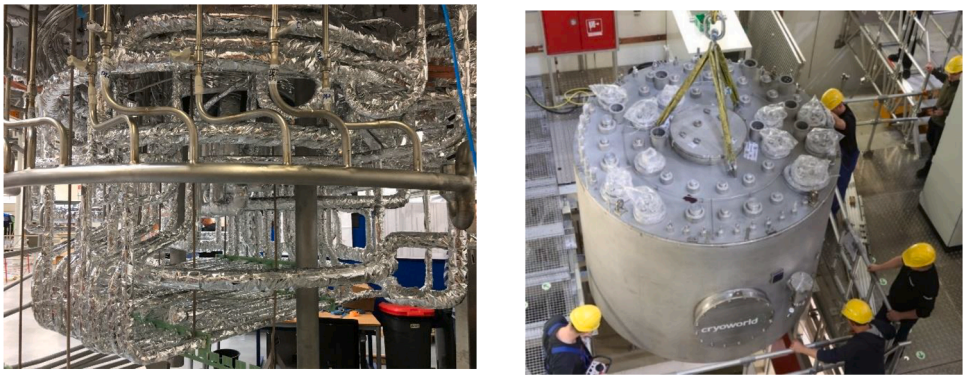

Fig. 7. Piping inside the cryo valve box (CBV) on the left side and view from above during the crane transport of the CVB in the W7-X torus hall

In order to address the high data rates produced by state-of-the-art cameras, a lossless video compression algorithm was developed together with collaborators from Google and integrated into the W7-X software infrastructure. The algorithm allows for a significant data rate reduction and is transparent to the user. Compression happens at the source and decompression is done within the API while reading data. Hence, the user does not even realize that data was losslessly compressed during transport and storage.

3.5. CoDaC infrastructure

The real-time control system had to be re-designed as well. The original VxWorks-based architecture was ported to a real-time linux infrastructure. When the system was originally designed in the early 2000's, multi-core CPUs did not exist, so dedicated operating systems like VxWorks were the only available basis for a deterministic control system. With multi-core architectures and the now existing implementations of real-time linux-based operating systems (e.g. concurrent RedHawk) a switch was without alternative in order to support the current requirements driven primarily by the divertor protection system. This system consists of more than 20 infrared cameras which monitor the emissivity of divertor and surrounding areas, calculate the temperature in real-time and trigger an interlock in case the temperature threshold is exceeded. The maximum total cycle time of the system from frame acquisition and all necessary calculation processes to switching off the heating systems is 100 ms. The required computing power and architecture of the system would have proven a challenge with the old VxWorks-based real-time system, but the lack of driver support for the cameras would have made it prohibitively expensive to implement. Instead, the real-time system was ported to linux and runs on RedHawk as RTOS, where drivers for the frame grabbers were readily available.

A further core component of the heart of the CoDaC infrastructure was also re-designed, the segment control system. The original design dating back 20 years did not consider the number of segment-controlled components required for a discharge in OP 2.1. This made significant changes in the underlying database architecture as well as the business processes (e.g. parameter transformations, consistency checks or distributed experiment preparation) of the segment control system necessary. As these changes affect the fundamental components, significant effort was required to propagate them through all components of the segment control system [29].

4. Commissioning

4.1. Functional safety, Interlock system

The central safety and interlock systems were completely redesigned during CP 2. A significant number of new requirements had to be implemented [28]. One of the lessons learned from the previous campaign which influenced the final design was that the use cases of machine commissioning and scientific operation are very different and require a number of different operating regimes for the safety system in

order to support parallel commissioning activities as best as possible.

The fast interlock system nearly doubled in scope due to the actively cooled divertor and inner wall. This required both a significant enhancement in terms of functionality as well as a complete change in hardware architecture. The combination of required speed and complexity of the algorithms involved made a move from a Boolean processor to a Siemens S-1500 class PLC necessary. This in turn required a full re-design and re-implementation of the system.

Both systems were completed on time and the safety system went through a validation in accordance with IEC 16511 requirements in early 2022 which was a necessary condition for the commissioning of W7-X to commence. The fast interlock system is progressively being validated as the appropriate commissioning discharges are available. This concerns in particular the IR-based divertor protection system.

4.2. Vacuum and baking

Pump down of Vacuum Vessel (VV) and cryostat started end of January 2022. No major leaks at the cryostat occurred. After repair of some leaks on the VV, commissioning of VV and cryostat could be completed on begin of March 2022 with achieving a final pressure of less than 1×10^{-4} Pa in the VV and approx. 2×10^{-2} Pa in the cryostat.

Baking of VV has been successfully performed in August 2022 (for vessel pressure plot for three Campaigns see Fig. 8). During and after baking no indications of a leak at VV could be detected. Due to the high number of new components installed in the vacuum vessel during MP2.1, more outgassing had to be removed in comparison to previous baking processes. A comparison of the current mass spectrometer plots to plots of the previous operation phases show very similar results. No water leaks at the up to 500 bolded water pipe joints (CF-connections) inside the VV could be detected. Finally, the remaining vessel pressure after cool down is at a level of 2×10^{-6} Pa and thereby slightly lower than in previous campaigns.

4.3. Cool down

The cool down of the super conducting magnet system and its support structures was carried end of April till May 2022 and followed the procedure that was developed for the first cool down in 2015 [3]. The cool down required about 4 weeks time and was done without major problems (see Fig. 9). The difference between inlet temperature (feed temperature) and the maximum structure or coil temperature was limited to 40 K and the cool down rate above 80 K was limited to 1 K/h. The cool down was practically limited by the maximum allowed temperature difference of 40 K. This temperature difference is the result of the limited mass flows through the different parallel cooling circuits and the temperature gradient within the massive cold structures. Below 80 K the heat capacity of stainless steel is decreasing significantly and the mass flow rate can be increased as the pressure drop falls with increasing helium density. The overall behavior of the cryostat with the magnet system during cool down was confirmed. So the temperature sensors and the thermal coupling between the components thus retained their properties.

4.4. Magnet system

The commissioning of the superconducting magnet system started with a high voltage test at room temperature and ambient pressure. After the cool down of the magnet system to 4 K a further high voltage test was successfully performed. One aim of the commissioning of the superconducting magnet system was to test the modifications made during the last maintenance phase. The magnet power supplies were equipped with new high precise current measurement devices and a new data acquisition and storage system. The magnet system was energized several time up to the nominal current and current accuracy and data transmission were successfully tested. In a second step the magnetic configurations, which were also be used in the previous operation phase were operated and the electrical, hydraulically and mechanical behavior was checked and compared with results from previous operation phases. The test confirmed the full availability of the superconducting magnet system for the upcoming operation phase. In addition to the superconducting magnet system W7-X is equipped with two normal conducting magnet systems, the trim coils and the control coils. Five trim coils are mounted at the outer surface of the cryostat and are used to influence the outermost plasma regions in order to enlarge the experimental flexibility. The coils have dimensions of up to 3.5×3.5 meters and are operated with current of up to 1950A [30]. The trim coil system was successfully re-commissioned by ramping up all coils to their nominal current, followed by a switch-off tests to check the safety system.

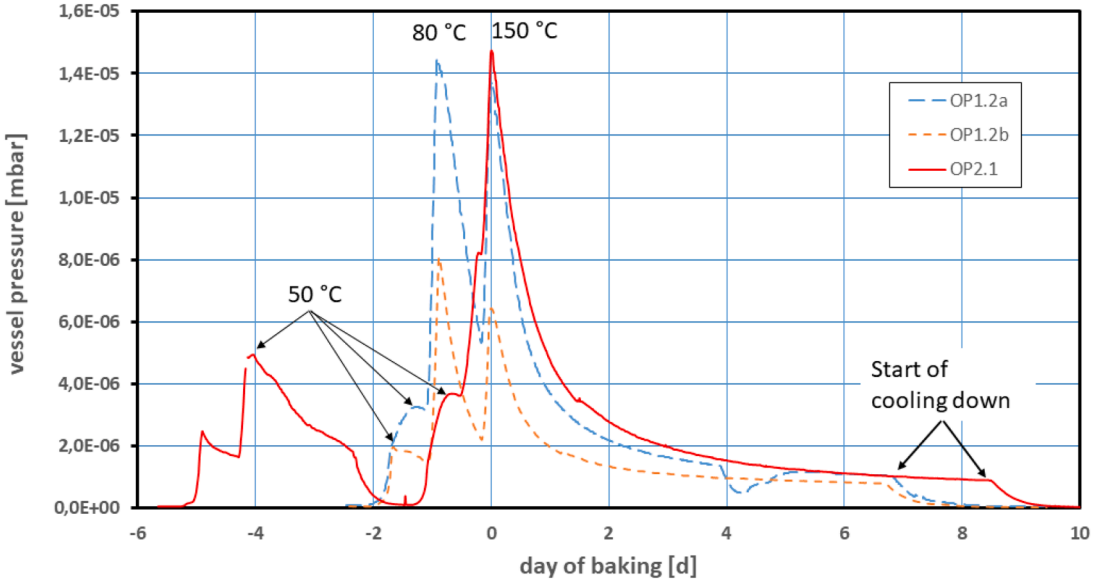

Fig. 8. Pressure of VV during baking, comparing three operation phases. After intermediate control points at 50°C and 80°C, the baking period of seven or more days starts with reaching 150°C inside the VV. The pressure at the end of baking is very similar for all commissioning processes, independent of the number of new installed components inside the VV. In OP 2.1 a pretest at 50°C was performed.

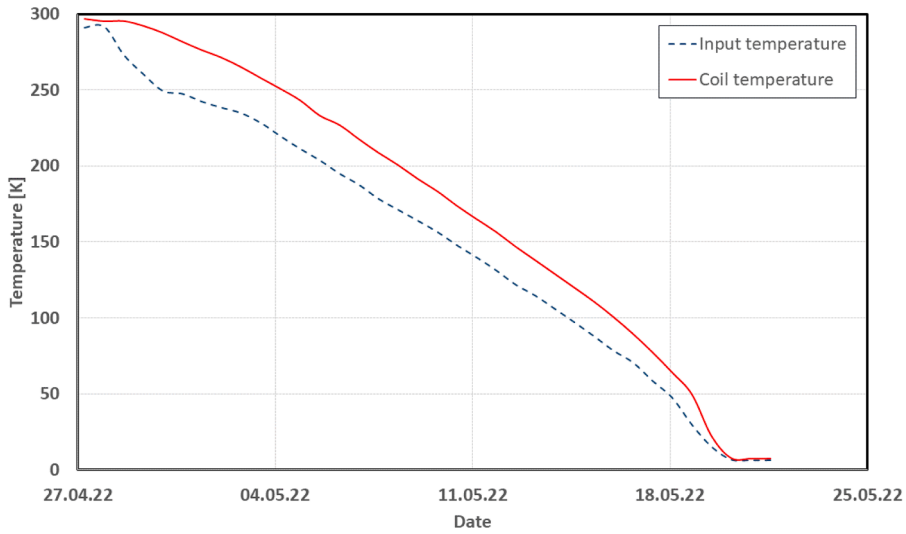

Fig. 9. Cool down of W7-X cryostat over time at start of OP2.1. A coil inlet temperature and corresponding coil outlet temperature are plotted over time. Temperature difference limits were respected.

The control coil systems consists of ten in-vessel-coils behind the divertor and is used e.g. to control the position and size of magnetic islands statically and/or dynamically. Therefore the power supplies can deliver dc current as well as ac current or combined dc+ac currents to the control coils [31]. The power supplies got a substantial upgrade during the last maintenance phase. In all ten units the driver boards of the high power electronics was new designed, produced and installed. The control system hardware was upgraded as well with new FPGAs. In summary the precision of the current was improved and the operation field could be enlarged.

4.6. Heating and fuelling

In order to fulfill the mission of W7-X, also additional heating and fueling systems are important.

As of now, the main heating is ECRH (10 x ~750 kW, at 140 GHz), but in the near future we expect a 1.5 MW gyrotron. All the gyrotrons are capable for 30 Min. pulses [32].

Neutral Beam Injection starts now with 4 (instead of 2 sources with 55 kV Hydrogen), i.e. 3.6 MW, for 5s [33].

An ICRH-system of 1 – 1.5 MW has been installed by FZJ/ERM recently [34].

A steady-state Pellet injector, provided in a collaboration with USA and Japan, is already in Greifswald but requires some preparation for the commissioning work. It is expected that this pellet injector will be operational only at the end of this experimental period [35].

4.7. Organisation of operation

The roles of the technical and Physics teams on W7-X have been established in the first operation phases [36]. The roles in the technical team (Engineer in Charge and Codac Operator) during operation have been altered to gain efficiency: Decision on bridging a safety action is done by the TLvD and implemented by the Operator. The official documentation during experimental days is now done by the Operator. Also the Physics team has now been stream-lined: The program leader oversees the collection and selection of experimental proposals and prepares and leads the daily experiment, together with the session leaders. The scientific program is divided into three Tasks forces: TFI Core scenario developmet, TFII Edge scenario development, TFIII Stellarator optimization.

For all the operation teams, the most important task is the protection of W7-X. Therefore, the instrumentation for the High Heat Flux Divertor and other sections of the first wall has been considerably extended and will be used to protect the divertor and walls from overheating. Real time thermography is an important player in this (see above in 3.4) but all data have to be brought together to monitor and control long plasma pulses [37].

Meanwhile more databases and tools to stream-line for the experimental operation have been established:

The data base of experimental proposal has been amended to derive the experimental program directly from the proposals

The magnetic configuration need, as discussed before, a thorough check on the mechanical stresses (i.e. FEM-calculations) and on electric behavior (as all power supply are connected). Therefore a database was established, where the configuration are checked and released online.

To cope with the growing number of integrated systems, the experiment program editor has been enhanced to assist distributed program preparation as a joint but coordinated task of the involved technicians and physicists.

Procedure to enhance the heating power energy (Power times shot length) has been extended in the number of input data. For any new magnetic configuration, the energy is increased in a sequence to check the heating of all in-vessel components. The main tool is the real time thermography, but temperatures measured in the plasma vessel and impurities in the plasma, are also part of the assessment, whether the energy can be increased any further in this magnetic configuration.

The main central control room has been modified to increase the number of work places, mostly for the steadily number of guests, participating in the W7_X experiments. For the scientific work, the number of working places was increased from 66 to 84, for the operation team from 8 to 12.Due to the Corona pandemic, however, the number of seats was reduced, in order to have sufficient distance between the colleagues.

5. Summary and outlook

Over the last years (2019-2022) W7-X underwent large modifications, which now make the device capable to fulfill its program, which is steady-state operation with high plasma energy. Also the further proof of the numerical optimization will go on.

The goal defined for the next experimental period, is an energy throughput of 1 GJ into the plasma. The first plasma in this configuration was performed on September 28, 2022.

Declaration of Competing Interest

The authors declare that they have no known competing financial interests or personal relationships that could have appeared to influence the work reported in this paper.

Data availability

Data will be made available on request.

Acknowledgement

This work has been carried out within the framework of the EUROfusion Consortium, funded by the European Union via the Euratom Research and Training Programme (Grant Agreement No 101052200 — EUROfusion). Views and opinions expressed are however those of the author(s) only and do not necessarily reflect those of the European Union or the European Commission. Neither the European Union nor the European Commission can be held responsible for them.

References

[1] J. Nührenberg, et al., Overview on Wendelstein 7-X Theory, Fusion Technol. 27 (1995) 71–78.
[2] H.-S. Bosch, et al., Construction of Wendelstein 7-X - engineering a steady-state stellarator, IEEE Trans. Plasma Sci. 38 (2010) 265–272.
[3] H.-S. Bosch, et al., Experience with the commissioning of the superconducting stellarator Wendelstein 7-X, Fusion Eng. Des. (2015) 22–27. **96-97**.
[4] R. Wolf, et al., Phys. Plasmas 26 (2019), 082504.
[5] T.Sunn Pedersen, et al., Phys. Plasmas 24 (2017), 055503.
[6] C. Beidler, Nature 596 (2021) 221.
[7] T.Sunn Pedersen, First divertor physics studies in Wendelstein 7-X, Nucl. Fusion. 59 (2019), 096914.
[8] A. Boozer, Nucl. Fusion. 61 (2021), 096024.
[9] H. Wobig and S. Rehker: A Stellarator coil system without helical windings. In: Proceedings of the 7th Symposium on Fusion Technology. Grenoble, France 1972, S. 345–353.
[10] P. Helander, Rep. Prog. Phys. 77 (2014), 087001 corrigendum 81, 099501 (2018).
[11] M. Landreman, E. Paul, Phys. Rev. Lett. 128 (2022), 035001.
[12] G. Grieger, et al., Fusion Technol. 21 (1992) 1767–1778.
[13] M. Jakubowski, et al., Overview of the results from divertor experiments with attached and detached plasnas at Wendelstein 7-x and their implications for steady-state operation, Nucl. Fusion. 61 (2021), 106003.
[14] T. Rummel, et al., Overview and status of commissioning of the Wendelstein 7-X magnet power supplies, IEEE Trans. Plasma Sci. 44 (2016) 1586–1591.
[15] A. Benito, D. Goitia, E. Casado, M. Andreres, E. Vázquez, M. Fajardo, C. Palacios, A. Cardella, D. Pilopp, L. Giodarno, G. Di Bartolo, Manufacturing of the coil support structure for W7-X, Fusion Eng. Des. 82 (2007) 1579–1583.
[16] A. Dudek, A. Benndorf, V. Bykov, S. Cardella, C. Damiani, A. Dübner, W. Dänner, M. Gasparotto, T. Höschen, G. Matern, Tests of critical bolted connections of the Wendelstein 7-X coils, Fusion Eng. Des. 82 (2007) 1500–1507.
[17] J. Reich, A. Cardella, U. Nielsen, R. Krause, H. Jenzsch, M. Bednarek, R. Kairys, G. Sobisch, and B. Vosslamber, "Manufacture of inter-coil support-elements of the W7-X magnet system," in Proc. 22th IEEE Symp. Fusion Eng., Albuquerque, NM, 2007, pp. 1–4.
[18] J. Geiger, et al., Plasma Phys. Control. Fusion 57 (2014), 014004.
[19] V. Bykov, A. Carls, J. Zhu, P. van Eeten, L. Wegener, H-S. Bosch, Mechanical monitoring issues in preparation to next step of Wendelstein 7-X operation, IEEE Trans. Plasma Sci. 46 (2018) 1086–1094.
[20] J. Zhu, V. Bykov, L. Wegener, H.-S. Bosch, Further Development of the W7-X magnet system finite element global model in preparation for enhanced operation phase, IEEE Trans. Appl. Supercond. 32 (2022), 4203106.
[21] A. Dinklage, et al., Nature Phys. 14 (2018) 855.
[22] T.Sunn Pedersen, et al., Nature Commun. 7 (2016) 13493.
[23] H. Renner, et al., Physical aspects and design of the Wendelstein 7-X Dicertor, Fus. Sci. Technol. 46 (2004) 318–326.
[24] R. Stadler, et al., The in-vessel components of the experiment WENDELSTEIN 7-X, Fus. Eng. Des. 84 (2009) 305–308.
[25] M. Nagel, M. Ihrke, M. Pietsch, H.-S. Bosch, C.P. Dhard, Th. Rummel, Concept for the cryo distribution for the Wendelstein 7-X cryo vacuum pumps, IOP Conf. Ser.: Mater. Sci. Eng. 502 (012109) (2019).
[26] G. Ehrke, B. Mendelevitch, J. Boscary, C. Li, R.J. Stadler, O. Sellmeier, P. McNeely, Design and manufacturing of the Wendelstein 7-X Cryo-Vacuum-Pump, Fus. Eng. Des (146) (2019) 2757–2760.
[27] F. Carovani, M. Pietsch, M. Nagel, Th. Rummel, H.-S. Bosch, Development, design and installation of multichannel transfer lines at W7-X under extreme geometrical constraints, Fusion Eng. Des., to be published.
[28] M. Nagel, C.P. Dhard, H. Bau, H.-S. Bosch, U. Meyer, S. Raatz, K. Risse, T. Rummel, Cryogenic commissioning, cool down and first magnet operation of Wendelstein 7-X, IOP Conf. Ser.: Mater. Sci. Eng. 171 (2017), 012050.
[29] A. Spring, et al., Establishing the Wendelstein 7-X steady state plasma control and data acquisition system during the first operation phase, Fus. Eng. Des. 123 (2017) 579–583.
[30] Th. Rummel, et al., The Wendelstein 7-X Trim Coil System, IEEE Trans. Appl. Supercond. 24 (2014), 4200904.
[31] F. Füllenbach, et al., Commissioning of the Wendelstein 7-X in Vessel Control Coils, IEEE Trans. Plasma Sci. 48 (2020) 2635–2638.
[32] V. Erckmann, et al., Electron cyclotron heating for W7-X: physics and technology, Fus. Sci. Technol. 52 (1977) 291–312.
[33] S. Lazerson, et al., First neutral beam experiments on Wendelstein 7-X, Nucl. Fusion. 61 (2021), 096008.
[34] J. Ongena, et al., Physics design, construction and commissioning of the ICRH system for the stellarator Wendelstein 7-X, Fus. Eng. Des. 192 (2023), 113627.
[35] S.J. Meitner, et al., Design of a continuous pellet fueling system for Wendelstein 7—X, IEEE Trans. Plasma Sci. 48 (2020) 1585–1590.
[36] P. van Eeten, H.-S. Bosch, R. Brakel, S. Degenkolbe, Organizing Wendelstein 7-X device operation, Fus. Eng. Design 160 (2020), 111843.
[37] A.Puig Sjtjes, et al., Real-time detection of overloads on the plasma-facing of Wendelstein 7-x, Appl. Sci. 11 (2021) 11969.